ELSEVIER

Marine Geology 188 (2002) 109–127

MARINE GEOLOGY
INTERNATIONAL JOURNAL OF MARINE GEOLOGY, GEOCHEMISTRY AND GEOPHYSICS

www.elsevier.com/locate/margeo

Late Weichselian iceberg, surface-melt and sediment production from the Eurasian Ice Sheet: results from numerical ice-sheet modelling

M.J. Siegert *, J.A. Dowdeswell [1]

Bristol Glaciology Centre, School of Geographical Sciences, University of Bristol, Bristol BS8 1SS, UK

Received 9 March 2000; accepted 25 February 2002

Abstract

Results from a numerical ice-sheet model were matched with geological evidence detailing the extent and timing of the Late Weichselian ice sheet in the Eurasian Arctic, through simple adjustments in the model's environmental inputs. The numerical model predicts the spatial and temporal variation in (1) subglacial sediment transport and deposition, (2) rates of iceberg calving and (3) rates of supraglacial melting over the past 30 000 yr. The ice sheet is characterised by a series of ice streams occupying bathymetric troughs in the Barents Sea and west of Norway, which act as sources for glacial sediment build-up and iceberg production. Our model indicates that significant volumes of sediment are deposited over the Bear Island fan (3000 km^3 in 12 000 yr), Franz Victoria Trough fan (500 km^3 in 8000 yr) and a series of smaller fans west of Norway (which combine to yield 4000 km^3 in 12 000 yr). The Norwegian Channel ice stream operated for only 4000 yr, during which time 400 km^3 of sediments were deposited on the adjacent fan. The ice sheet experienced two major periods of iceberg production where the rate of calving increased by ~50% at about 15 000 and 12 500 yr ago. However, the time-dependent response of iceberg calving to sea-level rise for individual ice streams is shown to be more complicated than the generalised ice-sheet response. The marine portions of the ice sheet decayed after 15 000 yr ago, resulting in several embayments at the mouths of bathymetric troughs. A second pulse of enhanced iceberg calving at 12 500 yr ago caused further decay of the marine ice sheet and the ice margin retreated back to the shorelines of island archipelagos in the northern Barents Sea. Ice loss through surface melting was restricted mostly to the southern margin of the ice sheet.

Keywords: Eurasian Arctic; Weichselian; deglaciation; modelling

1. Introduction

During the Late Weichselian, the Eurasian Ice Sheet covered the British Isles, Scandinavia, the Barents Sea and part of the Kara Sea (Landvik et al., 1998; Svendsen et al., 1999; Dowdeswell and Siegert, 1999). The timing and size of this major ice sheet have been much debated over the past 20 yr. Recent geological data and numerical mod-

[1] Present address: Scott Polar Research Institute and Department of Geography, University of Cambridge, Cambridge, CB2 1ER, UK.

* Corresponding author. Tel.: +44-117-928-8902; Fax: +44-117-928-7878.

E-mail address: m.j.siegert@bristol.ac.uk (M.J. Siegert).

0025-3227/02/$ – see front matter
PII: S0025-3227(02)00277-3

elling information have allowed the margins and ice thickness of this ice sheet to be evaluated with some confidence (Lambeck, 1995; Landvik et al., 1998; Dowdeswell and Siegert, 1999). Further, modelling has provided a time-dependent history of the Late Weichselian ice-sheet build-up (Siegert et al., 1999). However, information on the processes by which the ice sheet disintegrated, and the rate of ice-sheet decay resulting from those processes, have yet to be identified fully. In this paper, we present numerical modelling results on the break-up of the Late Weichselian Eurasian Ice Sheet, and the processes predicted to be responsible for this decay.

Glacial–geological information has been used to reconstruct the ice-sheet margins at the last glacial maximum (LGM) (Landvik et al., 1998; Svendsen et al., 1999) (Fig. 1a). These data have been acquired in recent years through two multidisciplinary ESF programmes named PONAM and QUEEN. At the LGM, the western margin of the Eurasian ice sheet was positioned along the continental margin from the North Sea, across western Scandinavia and the Barents Sea, along the northern margin of the Barents Sea to Severnaya Zemlya (Fig. 1a). The eastern margin of the ice sheet was located west of the Taymyr Peninsula, yielding an ice sheet and climate reconstruction at 16 000 yr ago as in Siegert et al. (1999) (Fig. 2). The position of the southern margin of the ice sheet has been established from well documented moraine sequences along the northern Russian and European mainland (Svendsen et al., 1999; Tveranger et al., 1995). The western and northern margins of the ice sheet were drained by fast-flowing ice streams with deformable beds which occupied submarine bathymetric troughs. The basal deforming sediments were transported along the line of ice flow to the continental shelf break, where they were deposited and built up as trough-mouth fans (Dowdeswell and Siegert, 1999).

Ice was lost from this ice sheet through (a) iceberg calving along the marine margins and (b) surface melting along the southern land-based margins of the ice mass. We are able to establish the time-dependent and spatial variation in the flux of ice lost through these processes by modelling the ice sheet over the period of its Late Weichselian growth and decay. In doing so, the flux of icebergs and meltwater to the Norwegian–Greenland Sea and North Atlantic from the Eurasian Ice Sheet is reconstructed. Model predictions of deglaciation are compared with two independent datasets. The first is the geologically inferred ice-sheet margin at three time slices during deglaciation (Fig. 1a) (Landvik et al., 1998), and the second is the rate of isostatic uplift measured across the Eurasian High Arctic (Fig. 1b) (Svendsen et al., 1999).

2. Numerical model

A simple ice-sheet model is coupled with a model describing the deformation and transport of water-saturated basal sediments. The ice-sheet model is based on the continuity equation for ice (Mahaffy, 1976), where time-dependent change in the ice thickness of a grid cell is associated with the specific net mass budget of a cell:

$$\frac{\partial h}{\partial t} = b_s(x,t) - \nabla.F(u,h) \tag{1}$$

where $F(u,h)$ is the net flux of ice from a grid cell ($m^2\ yr^{-1}$) (a function of the ice thickness, h, and velocity, u, of a cell and its neighbouring cells). In this investigation, the specific mass budget term, b_s, is related to the annual ice-surface accumulation/ablation and iceberg calving. Eq. 1 is solved using an explicit finite difference technique.

The depth-averaged ice-deformation velocity, u_i ($m\ s^{-1}$), is calculated by:

$$u_i \frac{2A\tau_b^n H}{n+2} \tag{2a}$$

where

$$\tau_b = \rho_i g h \sin(\alpha) \tag{2b}$$

where n is the flow-law exponent (equal here to 3), τ_b is the basal shear stress (Pa), ρ_i is ice density (870 kg m^{-3}), α is ice-sheet surface slope and g is acceleration due to gravity (9.81 m s^{-2}) (Paterson,

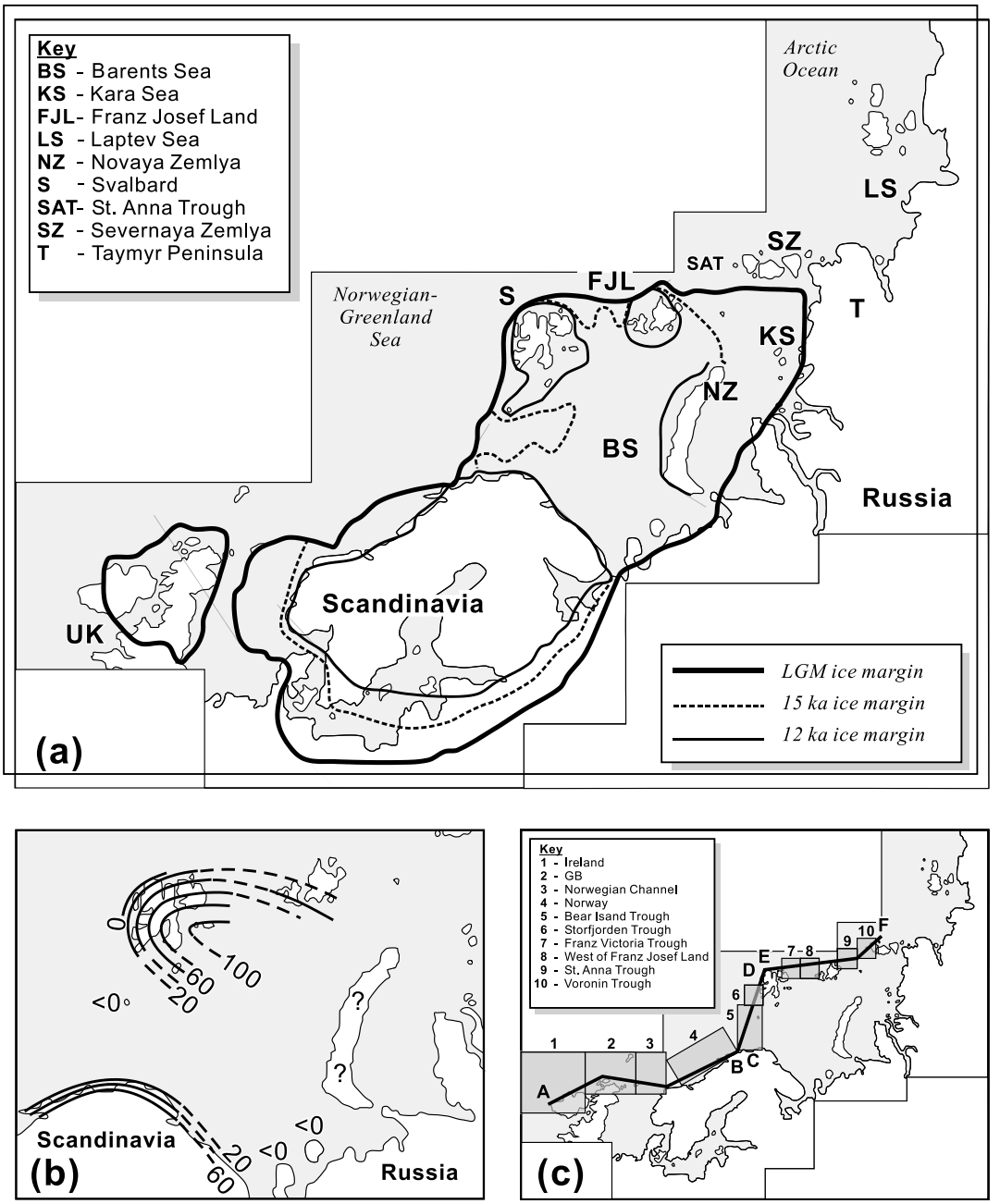

Fig. 1. (a) The location of the Eurasian Arctic and northwestern Europe. The map indicates the area of the model grid (which consists of 310×240, 20-km-wide cells). Also shown is the ice-sheet limit at three time slices determined from geological evidence (Landvik et al., 1998; Svendsen et al., 1999). The LGM refers to the maximum extent of ice, sometime between 21 000 and the onset of deglaciation. (b) Isostatic uplift curves across the Eurasian High Arctic at 10 000 yr ago. Contours (m) show the isobases in metres at 10 000 yr ago (adapted from Landvik et al., 1998). (c) Boxes denoting regions over which sediment delivery to the trough-mouth fans, rates of iceberg calving and surface melting were calculated. Also shown are three transects over which rates of sedimentation, iceberg calving and surface melting at four time slices are calculated (AB, CD, EF, Figs. 7, 9 and 10b).

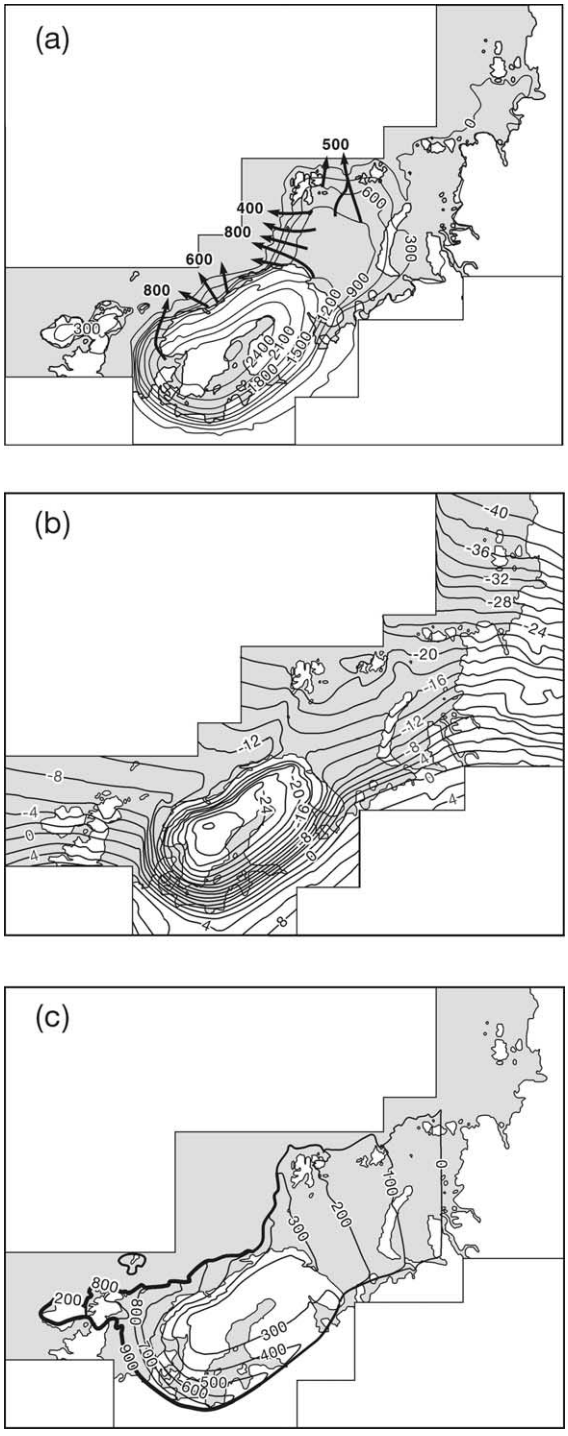

Fig. 2. The Eurasian Ice Sheet at 16 000 yr ago. (a) Ice surface elevation (m a.s.l.) and ice surface velocity (maximum velocity within ice streams is indicated, m yr^{-1}), (b) mean annual air temperature (°C), (c) mean annual accumulation of ice (mm yr^{-1}). Note that much the North Sea has a positive mass balance. However, no ice grows as a direct result here because the model assumes that the snow falls over open water. Adapted from Siegert et al. (1999).

1994). The mean ice temperature of a cell is set at −10°C, a temperature often used in isothermal ice-sheet models to determine the flow-law parameter A (5.3×10^{-15} kPa^{-3} s^{-1}; Payne et al., 1989; Dowdeswell and Siegert, 1999). As the ice-sheet model runs, the topographic grid is continually adjusted to account for ice-loading of the crust through a glacial cycle after the isostasy method developed in Oerlemans and van der Veen (1984).

The processes by which large-scale glacial sedimentation occurred over the Eurasian Arctic trough mouths during the Quaternary had the capacity to transport several thousand cubic kilometres of material within a few thousand years. Dowdeswell and Siegert (1999) assumed that the deformation and subsequent down-slope transport of water-saturated basal sediment is the major mechanism by which glacial sediments are transported to the ice-sheet margin on the scale required. The model describing sediment deformation beneath an ice sheet is adapted from Alley (1990). The model allows for the rapid deformation of basal till (which is coupled to till geotechnical properties and basal stresses) as a component of the total ice velocity. The velocity due to the deformation of water-saturated basal sediments, u_b (m s^{-1}), is determined by (Alley, 1990):

$$u_b = h_b K_b \frac{(\tau_b - \tau*)}{N^2} \quad (3)$$

where K_b is the till deformation softness (0.013 Pa s^{-1}), h_b is the deforming till thickness (m), and N is the effective pressure (Pa). The till yield strength, τ^*, is:

$$\tau* = N \tan(\varphi) + C \quad (4)$$

(Alley et al., 1989; Boulton and Hindmarsh, 1987), where C is the till cohesion coefficient

(4000 Pa), and tan(φ) is a dimensionless glacier-bed friction parameter (0.2) (Alley, 1990). The total velocity, u, is then the sum of the sediment deformation, internal ice deformation, and any contribution from basal sliding.

The bed-deformation process assumes that there is no change in the effective pressure, N, through the deforming till thickness, h_b. In addition, neither ploughing nor discrete shearing of the till is accounted for in the bed-deformation model (Alley, 1990). As in Alley (1990), longitudinal stresses are not calculated. The generation of subglacial till is controlled by:

$$t = K_t \frac{u_b}{h_b} N \quad (5)$$

where t is the thickness of till produced in 1 yr and K_t is abrasion softness (3×10^{-9} m Pa^{-1}).

Beneath Ice Stream B in West Antarctica, the thickness of the water-saturated sediments has been found through seismic reflection studies to be around 6 m (Blankenship et al., 1986). Since the sediment thickness in some areas of the Barents Sea is much greater than this (e.g. Elverhøi and Solheim, 1983; Vorren et al., 1990), allowance should be made for the deforming thickness within a large column of sediments. Dowdeswell and Siegert (1999) assumed that the thickness over which 'active' deformation occurs is 2 m. Ice velocity resulting from sediment deformation occurs when the sediment shears due to stresses induced by the overriding ice. Thus, a redistribution of the basal sediment will occur when the material deforms. This is modelled using a continuity equation for sediment flux, similar in form to Eq. 1 (Alley, 1990; MacAyeal, 1992). Just as the ice-shearing velocity observed on the ice-sheet surface has to be 'depth corrected' before it can be used to determine the flux of ice, so too does sediment deformation. As in MacAyeal (1992), we assume that the vertically averaged horizontal velocity is half the velocity at the ice/till interface.

Sensitivity experiments which examined the relationship between, first, the thickness of the deforming layer, and, secondly, the generation of new sediment and sediment supply to the continental margin were undertaken by Dowdeswell and Siegert (1999). Relatively large percentage changes ($\pm 40\%$) to the amount of sediment generated beneath the ice sheet did not affect greatly the rate of transport of basal sediment to the continental margin. Thus, the model of subglacial sediment delivery to trough-mouth fans is insensitive to the generation of new sediment, providing a relatively thin veneer of sediment exists across the Barents Shelf (as is the case at present). The second sensitivity test revealed that, by changing the thickness of the deforming sediment layer, the rate of supply of sediments to the Barents Sea margin was modified. In addition, the test showed that, by changing the thickness of the deforming layer, the volume of sediment supplied to trough-mouth fans is affected. However, the sensitivity results indicate that extremely large alterations ($> \pm 200\%$) to the deforming thickness were required to force model results to be incompatible with geological evidence of Late Weichselian sediment volume over fans. Because of this, it was concluded that the model of sediment supply to the continental margin used by Dowdeswell and Siegert (1999) was not adversely affected by significant variation ($\pm 50\%$) in a deforming sediment thickness of 2 m.

3. Model boundary conditions

3.1. Bedrock elevations

It is assumed that, at 30 000 yr ago, the bedrock elevation of the Eurasian High Arctic, Scandinavia, northern European mainland and the British Isles (and surrounding seas) was similar to that of today, allowing the present bedrock elevation to be used to define initial model conditions. The justification for this assumption is based on sedimentary evidence from central Svalbard and Scandinavia which indicates interstadial conditions between 50 000 and 30 000 yr ago, when glaciers were not significantly larger than at present (e.g. Mangerud and Svendsen, 1992). The bedrock elevation grid over which the ice sheet was constructed is composed of 74 400 square cells (310 north by 240 east), with a width of 20 km per cell. The bed elevations were derived from a series of

topographic and bathymetric maps (General Bathymetric Chart of the Oceans, Canadian Hydrographic Service, Ottawa, ON, Canada) and radio-echo sounding data on modern ice thickness and subglacial bedrock elevation (e.g. Dowdeswell et al., 1986).

3.2. Sea-level change and iceberg production

During periods of ice-sheet growth, global sea level falls due to the abstraction of water from the oceans to ice sheets. We use a eustatic sea-level curve for the last 30 000 yr to determine the time-dependent change in sea level (Fairbanks, 1989). Relative sea level is then determined by summing the eustatic sea level with the isostatically adjusted bedrock elevation.

A depth-related calving function is employed to describe the amount of ice removed from the marine margin of the ice sheet. The relation used is:

$$V_c = M[70 + 8.33h_w] \quad (6)$$

where V_c is the calving velocity (m yr^{-1}) and h_w is the water depth (m). This relationship has been deduced from a statistical analysis of calving glaciers from several polar locations, including Svalbard (Pelto and Warren, 1991). Hughes (1992) and Hanson and Hooke (2000) have outlined depth-related physical mechanisms by which glacier and ice-sheet calving might occur. Since the Eurasian Ice Sheet would have most likely been grounded at its marine margins, our use of a depth-related iceberg-calving algorithm can be justified. Nevertheless, there is a possibility that some sections of the ice-sheet margin were afloat in which case ice would also be lost via subglacial melting. Therefore our iceberg-calving rates should actually be regarded as 'marine ice-loss' rates, comprising iceberg calving and, to a much lesser extent, ice shelf melting.

A 'tuning' coefficient M is used to force the ice sheet to decay in a manner which is compatible with isostatic uplift curves derived from raised beach investigations (Siegert and Dowdeswell, 1995). This value is equal to 1 prior to 16 000 yr ago. However, after this time, the tuning parameter is doubled (as in Siegert and Dowdeswell, 1995). All other variation in the rate of iceberg calving is a result of changes in relative sea-level due to eustatic and isostatic effects.

3.3. Palaeoclimate forcing

The western margin of the Eurasian High Arctic has, in relation to its high latitude, an anomalously mild climate. This is due to relatively warm south-westerly prevailing winds which transfer heat and moisture from the Norwegian–Greenland Sea (Hisdal, 1985). The temperature of the Norwegian–Greenland Sea is influenced by the meridional Norwegian Current which transports relatively warm water from the North Atlantic. Eastward towards the Russian High Arctic, the climate becomes colder and drier (Dowdeswell, 1995). This climate gradient is illustrated by a mean annual air-temperature decline of 0.6–1.0°C per 100 km across the Svalbard archipelago (Simões, 1990).

The numerical model requires climatic inputs in the form of air temperature and precipitation, and their behaviour with respect to geographical location and altitude. However, there is a lack of continuous proxy records from which to infer the climatic history of the Eurasian High Arctic. To construct a simple palaeoclimate for the period of the last glaciation, a number of assumptions are made (as in Dowdeswell and Siegert, 1999). It is first assumed that, at present, the climate of the Svalbard–Barents Sea region is similar to the altitude–precipitation relationship defined as Polar Mix by Pelto et al. (1990), and that the climate over Scandinavia is defined as Sub-polar Mix, following Pelto et al. (1990). Secondly, if the present Barents Sea moisture source was curtailed, then a more continental-type precipitation regime would exist, similar to the Polar Continental (PC) altitude–precipitation relation in Pelto et al. (1990). Thus, the eastern Eurasian High Arctic is described by a PC-type relation.

In the numerical model, the equilibrium line altitude (ELA) is related to temperature through an environmental lapse rate typical for a large ice sheet of 5.1°C km^{-1} (Fortuin and Oerlemans, 1990). Thus, a temperature depression of 3°C will move the ELA downward by 600 m, such

that the ELA is numerically below sea level. Fleming et al. (1997), through surface energy-balance modelling of north–west Spitsbergen glaciers with a modern ELA of about 400 m, showed that a 3°C temperature change would shift the ELA below sea level, providing support for the simpler approach adopted here. Thus, through adjustments to the air temperature, the surface mass balance of the ice sheet can be adjusted.

In initial experiments, the air-temperature depression over the Barents Sea at the glacial maximum is set at 10°C (Manabe and Bryan, 1985). An assumption is made that, since glaciers on Svalbard were not significantly larger at 30 000 yr ago than today (Mangerud et al., 1992), the temperature conditions at 30 000 and 10 000 yr ago (the time at which Svalbard became largely ice free, and warm waters entered the Svalbard coastal region; Salvigsen et al., 1992), were similar to those at present.

There is a clear correlation between high-latitude palaeo-air temperatures (recorded in, for example, Greenland ice-core records) and indicators of global ice volume such as the global sea level, solar insolation, carbon dioxide, and oxygen isotope curves. Because of this, air-temperature change through time in the Svalbard–Barents Sea region can be calculated empirically by one of the three indicators of global ice volume (since the actual time function of air temperature is unknown for the Barents Sea region). Our results use the carbon dioxide forcing function (Barnola et al., 1987), but previous experiments have shown that there is little effect on ice-sheet size by selecting either sea level or oxygen-isotopic forcing functions (Siegert, 1993).

3.4. Geological data

There are three main geological datasets that act as boundary conditions for the numerical model. The first is ice marginal sediments detailing the maximum extent of the ice sheet (Svendsen et al., 1999). The second is geologically inferred ice-sheet limits across three time slices during deglaciation (after Landvik et al., 1998). These ice sheet limits plot the margin of the ice sheet's marine section at the LGM, 15 000 and 12 000 yr ago. The LGM and 12 000 yr limits are based on dated ice-marginal sedimentary sequences. The 15 000 yr limit is more tentative and is based on assumed rates of iceberg calving and ice-sheet break up (Landvik et al., 1998). The third geological dataset is the rate of ancient isostatic uplift measured across high Arctic archipelagos (Svendsen et al., 1999). This uplift is a function of the time-dependent change in ice loads during deglaciation.

In addition to these geological datasets, geophysical measurements of the sediment volume within trough-mouth fans across the margin of the western Barents Sea have been used to reconstruct the ice sheet in this region (Dowdeswell and Siegert, 1999). The ice sheet presented here is fully compatible with this sedimentary evidence.

4. Methodology

An inverse-type procedure is utilised in which the modelled ice sheet is forced to be compatible with independent geological datasets which reflect the LGM ice limit and manner of deglaciation. This forcing is controlled by adjustments to sea-level air temperature and the rate of iceberg calving as follows.

It is assumed that the spatial distribution of sea-level air temperature can be estimated through a series of temperature gradients. Our climate model has three main temperature gradients (a) from south–north (accounting for solar elevation change) (b) from west–east (due to distance from the relatively warm air over the Atlantic ocean) and (c) radiating from the central European continent as a consequence of solar heating of the land in the summer.

The first gradient establishes the southern limit of the ice sheet in the UK and Scandinavia, the second determines ice growth eastwards across the Kara Sea and Taymyr Peninsula, and the third defines the southern limit of the ice sheet across the Russian mainland. The air temperature is then adjusted to account for elevation above sea level using the lapse rate of 5.1°C km^{-1}.

These air temperatures then return to modern values at 10 000 yr ago through a linear relation-

ship with the carbon dioxide curve. The surface mass balance of the ice sheet is then calculated from air temperature using the temperature/mass balance relationship described earlier. Thus, the palaeoclimate at the LGM is estimated from considerations of the known LGM ice margin.

The rate of iceberg calving is governed by a water-depth-related algorithm. This algorithm involves a simple post-LGM tuning parameter which is used to ensure the marine sections of the Eurasian Arctic ice-sheet decay in a manner compatible with geological data. No other adjustments to the rate of iceberg calving are imposed on the model.

The model output provides time-dependent information on (a) ice-sheet dynamics (b) subglacial sediment delivery, (c) rates of surface melting and (d) rates of iceberg calving. Dowdeswell and Siegert (1999) used a similar procedure to determine rates of sediment supply to the continental margin of the Barents Sea.

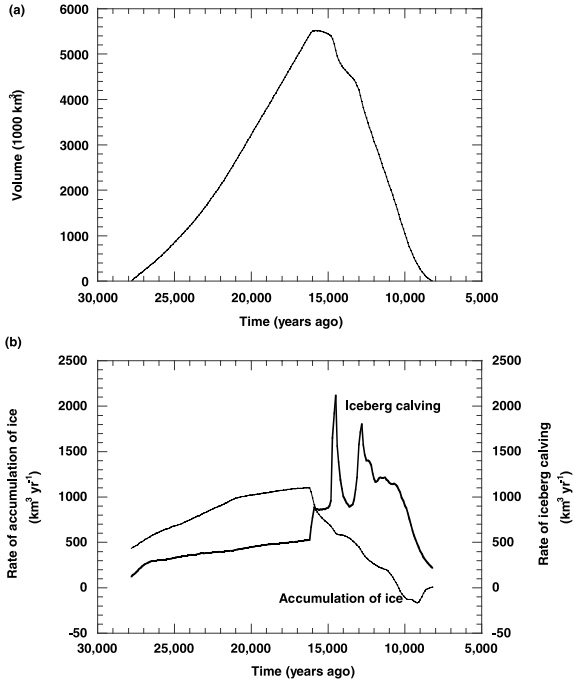

Fig. 3. (a) The volume of the Eurasian Ice Sheet (1000 km^3) over time. (b) Time-dependent rates of surface accumulation of ice and iceberg calving.

5. Model results

5.1. Ice sheet growth and decay

Ice-sheet initiation began 28 000 years ago as a result of ELA lowering across the Scandinavian mountains, Svalbard, Franz Josef Land and Novaya Zemlya (Fig. 3). Ice flow north from Scandinavia and south from Svalbard, in conjunction with eustatic sea-level lowering, caused the margin of the ice sheet to migrate into the Barents Sea. Complete glaciation of the Barents Sea by a grounded ice sheet was achieved by 20 000 yr ago. The ice sheet at its maximum size covered Scandinavia and the Barents Shelf. This ice sheet included a marine-based margin along the northern Barents Shelf, the western Barents Sea, western Scandinavia and northern Great Britain and Ireland. This ice-sheet margin contained a number of fast-flowing (>500 m yr^{-1}) ice streams located within bathymetric troughs between areas of relatively low ice velocity (Fig. 2). Although the western North Sea remains free of grounded ice in our reconstruction (Fig. 2a), we cannot rule out the possibility that the model under-predicts the extent of the ice sheet in this region, and that the Scandinavian and British Isles ice sheets were connected at the LGM.

The ice sheet reached its maximum size at 16 000 yr ago (Figs. 2a and 3a). The volume of this maximum ice sheet was $\sim$5 500 000 km^3. The ice sheet was configured such that a 2.7-km-thick ice dome existed over Scandinavia. Ice flowed south (towards its land-based margin in northern Europe), west to the North Sea and Norwegian Sea and north into the Barents Sea. The southern margin of the ice sheet was located across the northern margin of the Russian and European mainland. The extent of the ice sheet matches well with geologically derived ice limits (Svendsen et al., 1999). The construction of this LGM ice sheet is detailed in Siegert et al. (1999) and in (Fig. 1). The maximum ice thickness in the Barents Sea at 16 000 yr ago was around 1 km. Ice flow was organised from the central Barents Sea towards the continental margin as a series of fast-flowing ice streams which occupied bathymetric troughs (Fig. 2).

Deglaciation occurred as a response to sea-level rise and increased mean annual temperature. Sea-level rise, in conjunction with isostatic depression, caused an increase in the water depth at the marine margin and, hence, an increase in the rate of iceberg calving (Eq. 6). At the same time, increased surface air temperatures caused the elevation of the ELA along the southern margins of the ice sheet to rise, leading to surface run off of water.

The marine sections of the ice sheet deglaciated first. For example, by 14 000 yr ago some of the deeper bathymetric troughs such as the Bear Island Trough had deglaciated, forming large embayments of ice around the bathymetric feature (Fig. 4a,b). By 13 000 yr ago, the Bear Island Trough ice-free embayment had enlarged such that it covered the southern half of the Barents Sea. A second pulse of enhanced iceberg calving at 12 500 yr ago resulted in grounded ice becoming limited to the relatively shallow seas around archipelagos (Fig. 4c). As sea-level rise continued, the western and northern margin of the ice sheet was subject to increasingly high rates of iceberg calving, causing thinning of the ice sheet and its eventual decay by 10 000 yr ago. Meanwhile, the southern margin of the ice sheet was subject to surface melting, causing the ice front to retreat northwards towards Scandinavia. By 10 000 yr only a small ice cap existed over Scandinavia,

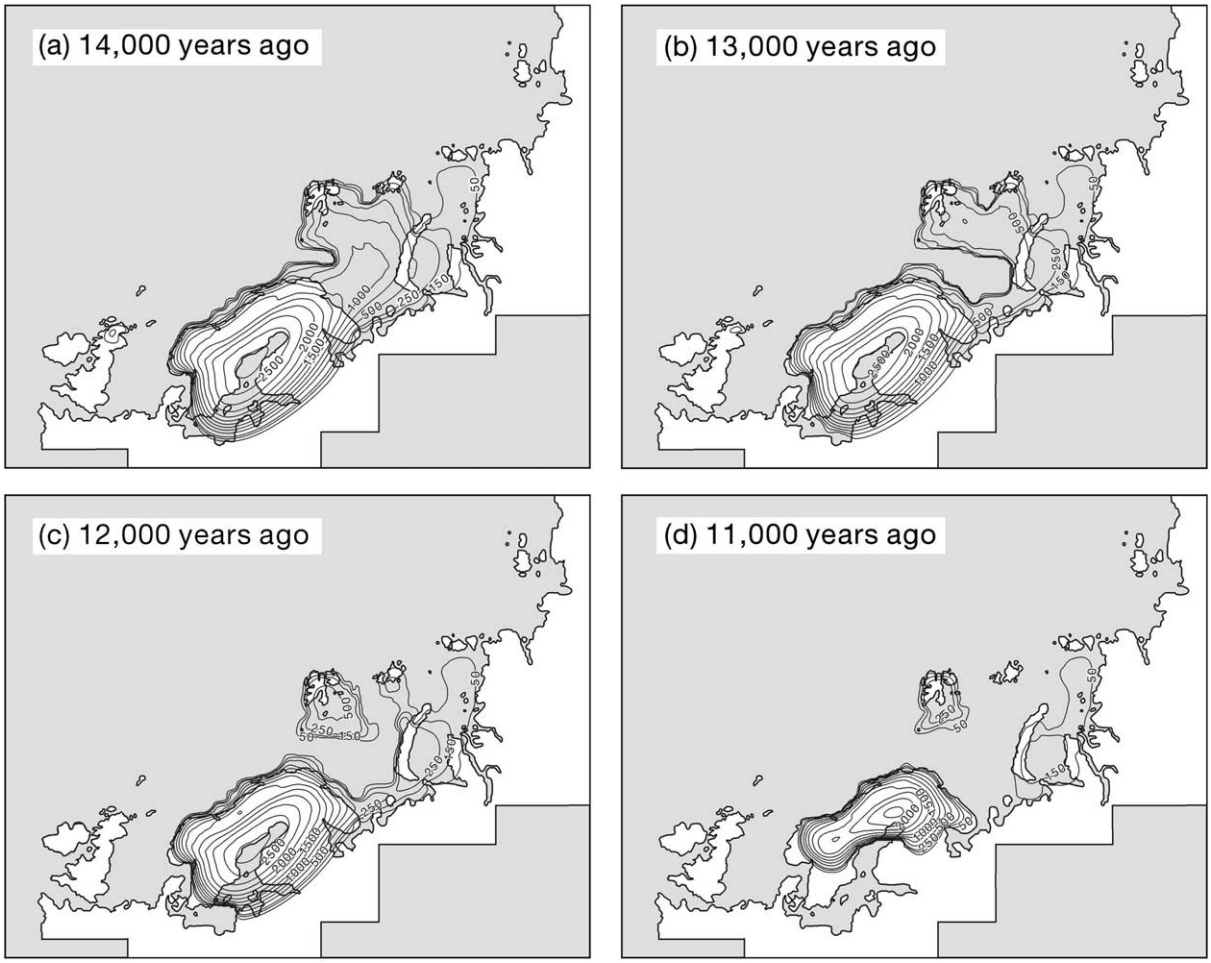

Fig. 4. Ice-sheet thickness at (a) 14 000 yr ago, (b) 13 000 yr ago, (c) 12 000 yr ago, (d) 11 000 yr ago. Contours are in metres.

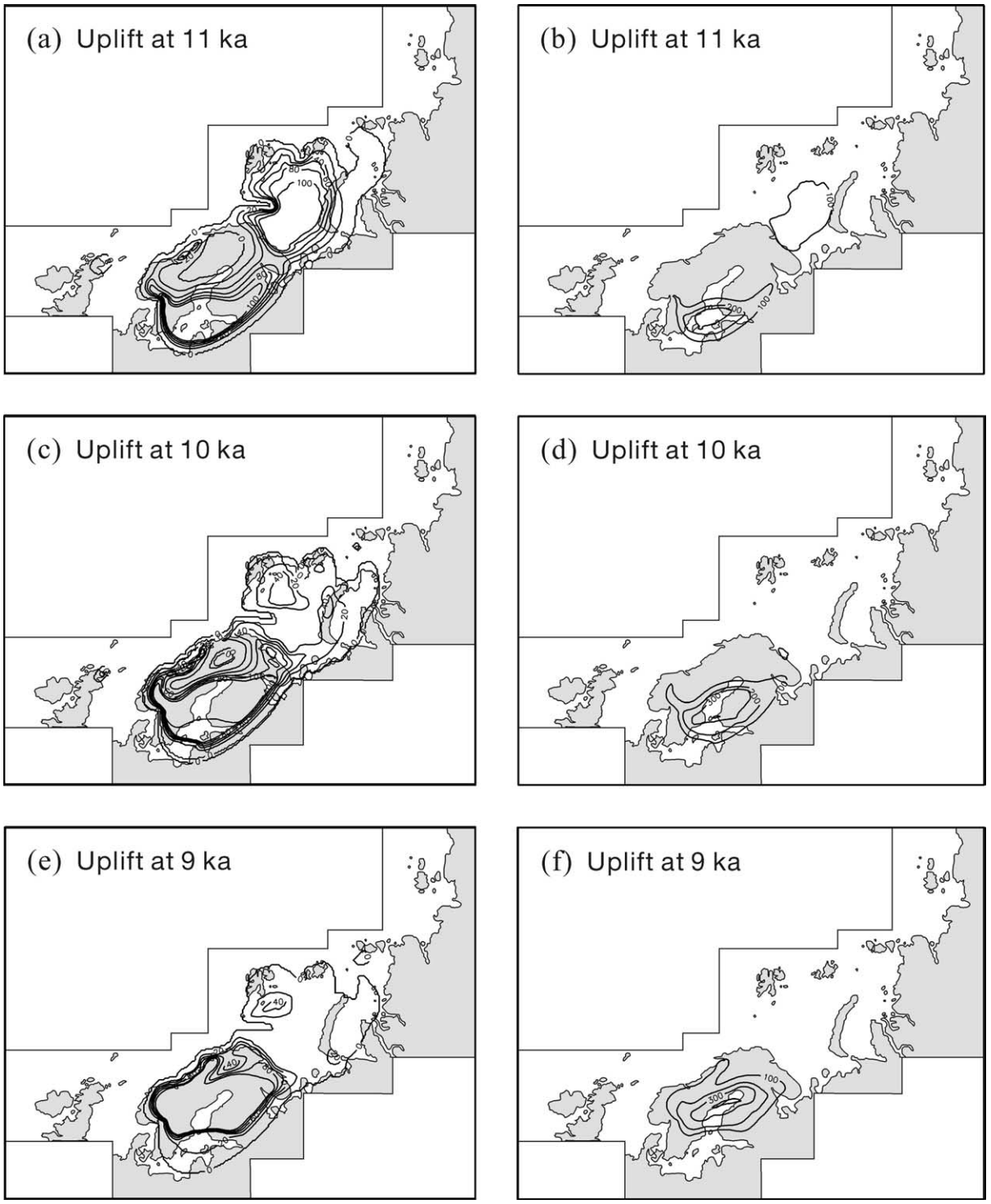

Fig. 5. Rate of bedrock uplift at (a,b) 11 000 yr ago, (c,d) 10 000 yr ago, and (e,f) 9000 yr ago. Note that (a), (c) and (e) show contours in 20 m/1000 yr up to 100 m/1000 yr, and (b), (d) and (f) display contours at 100 m/1000-yr intervals.

with other remnants of ice across Svalbard, Novaya Zemlya and Franz Josef Land.

5.2. Post-glacial isostatic uplift

The ice-sheet distribution during deglaciation controls the rate of isostatic recovery (Fig. 5). The isostatic pattern produced by our ice-sheet model is compatible with measured uplift patterns and rates at ~10 000 yr ago across the High Arctic (Forman et al., 1997; Svendsen et al., 1999), which indicate the emergence of the high Arctic archipelagos (Figs. 1b and 5c,d). Our model of post-glacial uplift also compares well with previous solid-Earth models of the isostatic response to deglaciation across Scandinavia (e.g. Fjeldskaar, 1991, 1994).

At 11 000 yr ago uplift contours around northern Scandinavia are parallel to the coast, whilst across Svalbard and Franz Josef Land they indicate a former centre of ice loading in the central Barents Sea (Fig. 5a,b). By 10 000 yr ago, the uplift patterns across Svalbard and Franz Josef Land reflect the decay of ice across the northern Barents Sea (Fig. 5c,d). This pattern is very similar to that measured from raised beaches at this time (Forman et al., 1997). By 9000 yr ago, isostatic uplift across Scandinavia is predicted to be centred over the Gulf of Bothnia, as it is today (Fig. 5e,f).

5.3. Transport of glacial sediments

Fast flow of ice within bathymetric troughs occurs in our model as a result of the deformation of water-saturated unconsolidated sediments at the base of the ice sheet. Deformation of subglacial material leads to its transport along the direction of ice flow. This process was active beneath the Barents Sea sections of the Eurasian Ice Sheet, and caused the transport of subglacial sediments along ice streams to the continental margin where they were either deposited or entrained within icebergs.

We predict sediment deposition at the continental margins by calculating sediment transport across a series of transects located close to the marine edge of the ice sheet (Fig. 1c). The first transect is located across western Ireland, northern Great Britain and west of Norway (A–B in Fig. 1c). The second is positioned at the western margin of the Barents Sea (C–D in Fig. 1c). The third transect is across the northern margin of the Barents Sea (E–F in Fig. 1c). We also inspect the model results by plotting the time-dependent variation in sediment volume at the mouths of bathymetric troughs (areas 1–10 in Fig. 1c).

Very little sediment is transported to the ice-sheet edge across the transect west of Ireland or over northern Great Britain (Fig. 7a). However, at the mouth of the Norwegian Channel, an ice stream which existed between 17 500 and 14 500 yr ago delivered up to 3 cm yr^{-1} of sediment to the continental margin (Fig. 7a). A total of 500 km^3 of sediment is calculated to have been delivered to the Norwegian trough-mouth fan during the Late Weichselian (Fig. 6a). West of Norway, a series of

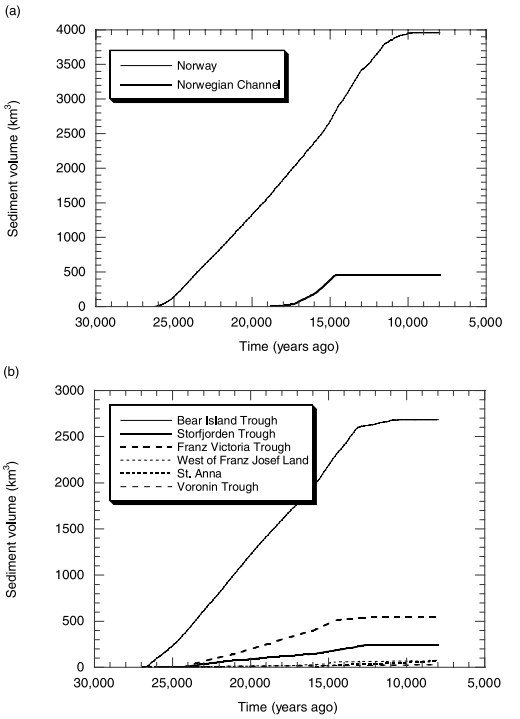

Fig. 6. The volume of sediment transported to several regions (defined as blocks in Fig. 1c) within the Eurasian Arctic during the Late Weichselian; (a) Norwegian Channel and west of Norway; (b) several troughs along the western and northern Barents continental margin (including the Bear Island, Storfjorden and Franz Victoria troughs).

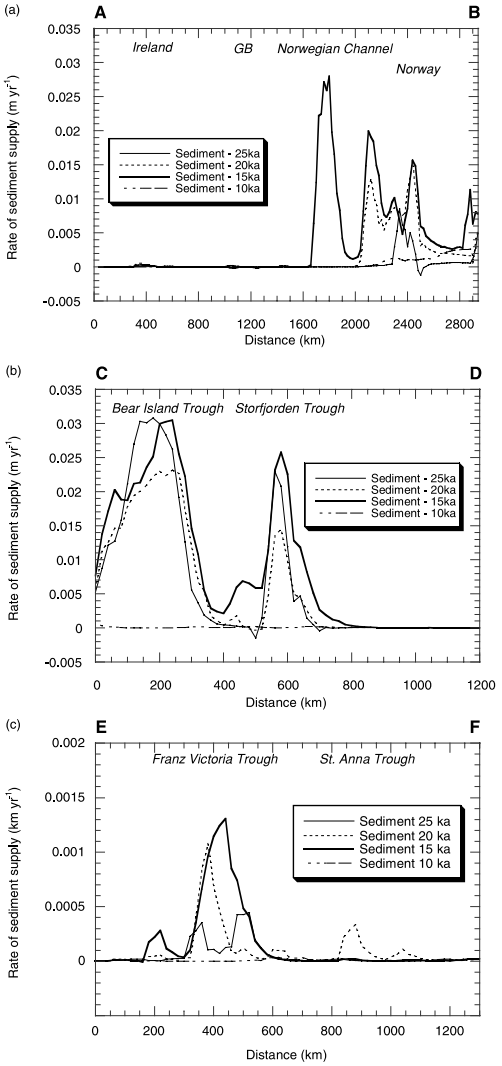

Fig. 7. Flux of sediment calculated across a series of transects (defined in Fig. 1c) across the Eurasian Arctic at four time slices (25 000, 20 000, 15 000, and 10 000 yr ago). (a) AB: Western Ireland, northern Great Britain, Norwegian Channel and western Norway; (b) CD: Bear Island, Storfjorden and western Svalbard; (c) EF: northern Barents continental margin (including Franz Victoria and St. Anna troughs).

relatively small troughs were occupied by ice streams between 23 000 and 12 000 yr. These ice streams transported 4000 km^3 of sediment to the continental shelf break over this longer period (Figs. 6a and 7a).

The transect across the western Barents Sea margin illustrates glacial sedimentation from the Bear Island Trough and the Storfjorden Trough ice streams. The ice streams were active from 25 000 to 14 000 yr ago. During this time, around 3000 km^3 of sediment was transported beneath the Bear Island Trough whilst for the Storfjorden Trough the volume of sediments was 250 km^3 (Fig. 6b). These model-predicted volumes compare well with geophysical measurements of Late Weichselian sediment volumes at the mouths of these troughs (e.g. Dowdeswell and Siegert, 1999).

Several modelled ice streams within bathymetric troughs across the northern, Arctic Ocean margin of the ice sheet led to the transport of sediments across our third transect (Fig. 1c). For example, the Franz Victoria Trough had an ice stream within it between 24 000 and 13 000 yr. The rate of sedimentation at the continental margin was between 1 and 1.5 cm yr^{-1} across the northern Barents Sea transect (Fig. 7c). This sedimentation led to the build-up of about 500 km^3 of material at the continental margin in front of the Franz Victoria Trough (Fig. 6b). Little sediment is predicted to be produced east of Franz Josef Land, due to a lack of significant ice build-up in the Kara Sea (Figs. 2a and 4a). Our model may under-predict the size of the ice sheet in this region, since there is some geological evidence for grounded ice within the St. Anna Trough (e.g. Polyak et al., 1997).

5.4. Production of icebergs

Our ice-sheet model is linked to a number of geological datasets which provide a 'calibration' for ice-sheet decay. We can therefore use the model to determine the rates of iceberg calving and melting required to force the ice sheet to be compatible with the geological conditions. We predict the rate of iceberg calving across the whole ice-sheet margin and over regions where large ice streams occur in the model (Figs. 1, 8 and 9). Our results show the spatial and temporal variations in iceberg production along the ice-sheet margins. Before the results are discussed, two characteristic features should be explained. The first is that iceberg calving increases gradually across the marine ice-sheet margins due to an in-

crease in ice thickness at the margin during ice-sheet growth, and a relative sea-level rise caused by isostatic depression of the Earth's crust. The second point is that, after 18 000 yr ago, (a) relative sea-level rise is enhanced by eustatic sea-level rise and (b) an increase in the iceberg-calving algorithm coefficient (M) at 16 000 yr is required to cause decay of the ice sheet in a manner compatible with measured post-glacial isostatic uplift patterns. This leads to large-scale iceberg-calving events during deglaciation, and the stepwise decay of the ice sheet.

Iceberg production occurred across all regions of the marine margin, but was greatest at the mouths of ice streams. For instance, the rate of iceberg calving west of Ireland increased from zero at 25 000 yr ago to 20 km^3 yr^{-1} at 16 000 yr ago. The rate of iceberg calving then returned to zero by 13 000 yr ago (Fig. 8). Thus, from the western Irish continental margin, only ~40 000 km^3 of icebergs were released into the ocean over 10 000 yr.

North of Great Britain, iceberg calving in-

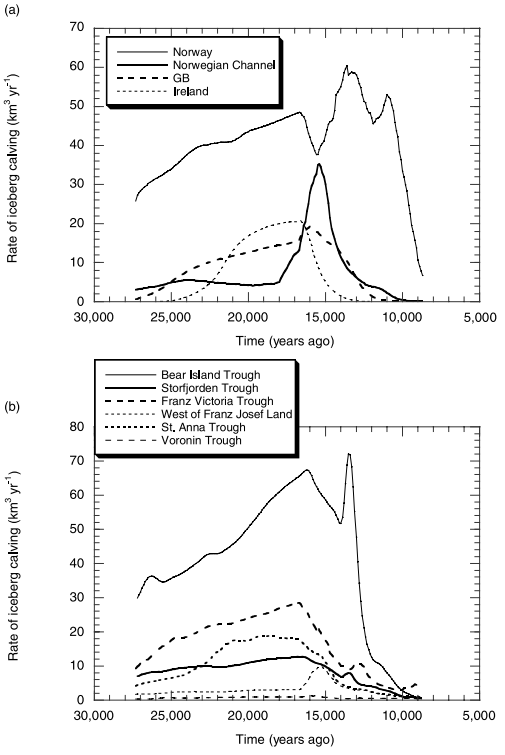

Fig. 8. The rate of iceberg production in several regions at the ice-sheet margin (defined as blocks in Fig. 1c) within the Eurasian Arctic during the Late Weichselian: (a) Ireland, Great Britain, Norwegian Channel and Norway; (b) several troughs along the western and northern Barents continental margin (including the Bear Island, Storfjorden, Franz Victoria and St. Anna troughs).

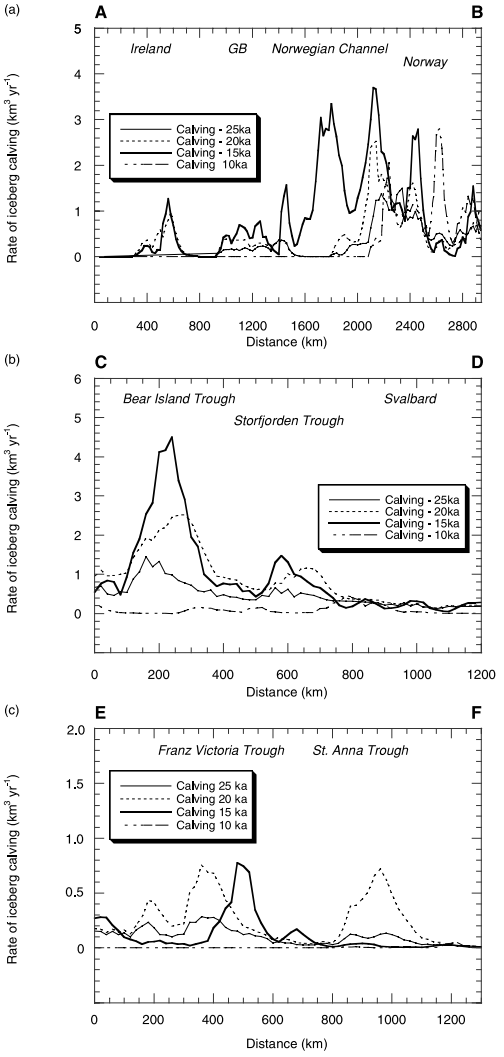

Fig. 9. Flux of icebergs calculated across a series of transects (defined in Fig. 1c) across the Eurasian Arctic at four time slices (25 000, 20 000, 15 000, and 10 000 yr ago). (a) AB: Western Ireland, northern Great Britain, Norwegian Channel and western Scandinavia; (b) CD: Bear Island, Storfjorden and western Svalbard; (c) EF: northern Barents continental margin (including Franz Victoria and St. Anna troughs).

creased relatively steadily along the marine margin between 25 000 and 16 500 yr (Figs. 8a and 9a). At 16 500 yr ago the rate of iceberg production from this ice margin increased from 10 to 20 km^3 yr^{-1} in about 5000 yr, due to sea-level rise. The rate of iceberg calving reduces to 0 by 12 000 yr ago (Fig. 8a).

The Norwegian Channel Ice Stream was active for a relatively short time, between 17 500 and 14 500 yr ago, and led to a significant flux of ice delivered to the shelf edge, where calving proceeded across the 200 km width of the trough mouth (Fig. 1). The peak rate of icebergs produced was 35 km^3 yr^{-1}, which lasted between 16 000 and 14 500 yr (Fig. 8a). After this time, the ice stream decayed and iceberg calving was halted.

A series of ice streams west of Norway, which were present between 25 000 and 12 000 yr, caused a significant volume of icebergs to calve into the Norwegian Sea. Nowhere along the transect west of Norway did the rate of iceberg calving exceed 4 km^3 yr^{-1} (Fig. 9a). However, collectively, the ice-sheet margin across this transect contributed as much as 70 km^3 yr^{-1} of icebergs to the open sea. The time-dependent variation in calving along this margin shows a decrease in the production of icebergs at 17 000 yr (as the ice margins retreat to shallower water). The rate of iceberg calving then increased from 40 to 60 km^3 yr^{-1} by 14 000 yr ago (Fig. 8a). This rate then reduced steadily to 50 km^3 yr^{-1} until 12 000 yr ago, after which the rate of iceberg calving increased again as the marine part of the ice sheet experienced final decay. This decay left an ice sheet limited to the Scandinavian mainland (Fig. 4d).

The remaining sections of the model transect in Fig. 1c deal with the margins of the marine-based Svalbard–Barents Sea ice sheet. Along the western margin, the dominant supply of icebergs was across the mouths of the Bear Island Trough and the Storfjorden Trough (Figs. 8b and 9b). For the Bear Island Trough, the rate of iceberg calving increased from 20 to 70 km^3 yr^{-1} between 25 000 and 16 000 yr ago. This steady increase in iceberg calving was due to (a) an increase in the ice thickness at the ice-sheet margin during ice-sheet build up and (b) post-LGM sea-level rise during ice-sheet decay. Note that two iceberg-calving events are recorded, at 16 000 and 13 500 yr ago. The iceberg-production rate shown in Fig. 8 represents all icebergs calved within a 5000 km^3 area of the ice sheet; not necessarily at the continental margin (Fig. 1c). Thus, as the ice sheet retreats across the Barents Sea, iceberg calving is still recorded in the Bear Island Trough region. The iceberg-calving history for the Storfjorden Trough is different to the Bear Island Trough in that the rate of calving increases gradually from 8 to 10 km^3 yr^{-1} between 25 000 and 15 000 yr (Fig. 8b). The rate of iceberg calving then declined as the thickness of ice at the ice-sheet margin reduced. An iceberg-calving event at 12 500 causes a brief (1000 yr) return to a calving rate of 70 km^3 yr^{-1} across the Bear Island Trough which is induced by sea-level rise at this time.

The northern Barents, Arctic Ocean margin of the Late Weichselian ice sheet is characterised by a major calving zone at the mouth of the Franz Victoria Trough (Fig. 8b). However, two smaller troughs along the northern Barents margin are also sites of enhanced iceberg calving (Fig. 1c). These sites together account for the majority of icebergs calved from the northern margin of the Late Weichselian ice sheet. The Franz Victoria Trough ice stream issued 25 km^3 yr^{-1} of icebergs at 16 000 yr ago. The rate of iceberg production increased steadily from 10 km^3 yr^{-1} at 25 000 yr ago (Fig. 8b). This rate was reduced to about 10 km^3 yr^{-1} at 14 000 yr and to zero by 10 000 yr ago as the ice sheet decayed. The two smaller troughs along the northern Barents margin contributed 5 km^3 yr^{-1} of icebergs at 15 000 yr.

The spatial pattern of LGM iceberg-calving rates along the western Barents and Scandinavian margins match well with those predicted independently by Bigg et al. (1998). This adds a level of support to the LGM ice-sheet configuration (Fig. 2a; Siegert et al., 1999).

It is interesting to note that the maximum amount of iceberg production correlates to the most active phase of deglaciation. This is also seen in the records of iceberg-rafted debris in the Norwegian–Greenland Sea (Baumann et al., 1995; Dowdeswell et al., 1999). Our predictions of iceberg production in time and space show a

dynamic response to sea-level rise at different places and times around the ice sheet. Thus, the rate of ice-sheet decay from calving varied around the ice sheet during deglaciation (Fig. 9). When these dynamic calving responses are placed together, their respective signals interfere with each other to produce two major calving peaks which dominate the calving signal from the ice sheet as a whole (Fig. 3).

5.5. Surface meltwater

Meltwaters from the Eurasian Ice Sheet are produced in our model when the ELA rises above the elevation of the ice surface. This situation is predicted to occur across the ice sheet in Ireland and Great Britain, and along the southern margin of the ice sheet in northern Europe. Our model forced the LGM ice sheet to match the location of moraine ridges along the southern margin of the ice sheet by raising the surface air temperature and, hence, the ELA. The ice sheet responds by the ablation of ice at this margin. If the flux of meltwater is less than the flux of ice in ice-marginal grid cells, ice advance occurs. If the flux of meltwater is greater than the flux of ice, glacial retreat is modelled. We analyse the meltwater released by the Eurasian Ice sheet by dividing the ice sheet margin into a number of melt zones (Ireland, Great Britain, the Norwegian Channel Ice Stream and western Norway, and a zone covering the whole ice sheet; Fig. 10).

In Ireland, surface melting of the ice sheet was the dominant ice-loss term during the last glaciation. The rate of melting increased from 1 km^3 yr^{-1} at 20 000 yr to 15 km^3 yr^{-1} at 14 000 yr when the ice sheet was modelled at less than 50 m thick (Fig. 10). For the northern margin of the British Ice Sheet, melting reached a maximum of 7 km^3 yr^{-1} at 12 000 yr ago. This rate then reduced as the ice sheet decayed by 11 000 yr ago (Fig. 10). There was very little surface melting of the Norwegian Channel ice stream, as it had decayed before the equilibrium line rose above the ice surface. However, at 10 000 yr ago, a relatively small ice cap over western Scandinavia was melted at a rate of 10 km^3 yr^{-1} for 1500 yr (Fig. 10).

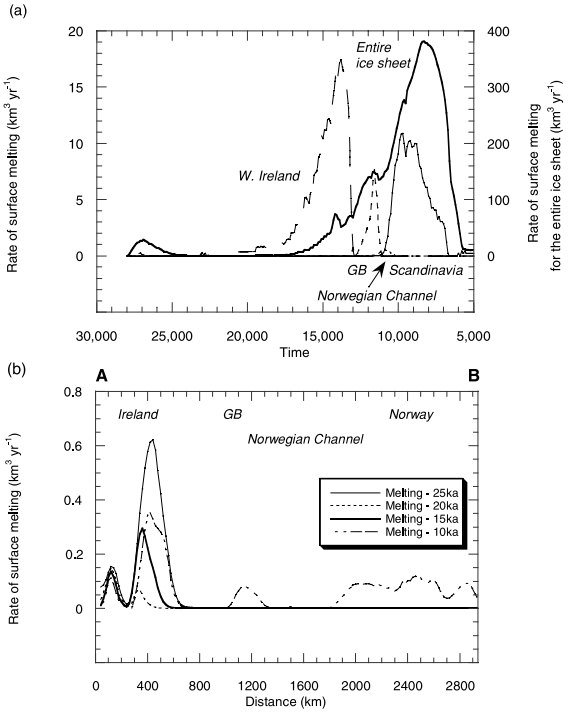

Fig. 10. (a) Time-dependent variation in the volume of surface meltwater produced across several regions (defined as blocks in Fig. 1c) of the Eurasian Ice Sheet during the Late Weichselian. The time-dependent volume of surface water melted from the entire ice sheet is also indicated (note the different *y*-axes). (b) Flux of meltwater calculated at four time slices (25 000, 20 000, 15 000, and 10 000 yr ago) across AB: Western Ireland along the northern Great Britain and the Norwegian Channel to western Scandinavia (Fig. 1c).

The land-based southern margin of the Eurasian Ice Sheet (i.e. the southern Barents Ice Sheet, and the south-eastern sector of the Scandinavian Ice Sheet) was characterised by large-scale melting throughout the deglacial phase. The time-dependent rate of surface melting is related to the height of the ELA over time across this margin. Our model calculates the flux of surface melt required to produce the ice-sheet edge located at the moraine features marking the ice sheet terminus (Svendsen et al., 1999). Prior to the LGM, very little melting occurs along the margin. During deglaciation, however, as the ELA rises due to air-temperature increase, the southern margin of the ice sheet becomes a zone of surface ablation. Our

calculations show that the ice sheet lost around 1 500 000 km^3 of ice through surface melting between 15 000 and 8000 yr ago (Fig. 10). We calculate that around 90% of this water originates from the southern land-based margin of the ice sheet.

6. Sensitivity tests

Several experiments have been undertaken previously to examine the sensitivity of the ice-sheet dimensions to changes in environmental inputs used to force the model (Siegert et al., 1999). Inputs controlling directly the mass balance of the ice sheet (i.e. rates of accumulation and iceberg calving), and the maximum sea-level depression, were adjusted by a maximum of ±10% of the standard value. The entire ice sheet was subject to variations in model inputs. Although the ice-sheet dimensions are most sensitive to alterations in the imposed environmental conditions, relatively large (±10%) changes in the inputs of accumulation, iceberg calving and sea level do not adversely affect the main results and conclusions of the reconstruction of the Eurasian Ice Sheet given in Siegert et al. (1999). Furthermore, significant changes (±10%) in the dynamics of the ice-sheet model (i.e. parameters relating to the calculation of the flow of ice and the deformation of basal sediment) produced smaller ice-volume variations than the sea-level depression experiment (Siegert et al., 1999).

7. Supply of meltwater and icebergs to the ocean

From our numerical model, we are able to understand the time-dependent history of iceberg calving and meltwater production in relation to the formation and break up of the last Eurasian Ice Sheet. Cooling of the air temperature prior to 18 000 yr ago induced a relative lowering of the ELA from modern-type values at 30 000 yr ago, which encouraged ice growth across Scandinavia and Great Britain and along the northern coast of mainland Europe. Deglaciation in these regions was triggered by air-temperature rise which elevated the ELA, causing melting and retreat of the ice-sheet margin northwards. Thus, the maximum rate of meltwater production was during deglaciation. As deglaciation continued, the ELA rose in more northern locations (e.g. northern Scandinavia and the Barents Sea). Because of this, the focus of meltwater delivered to the open ocean would have shifted northward from Ireland at 15 000 yr ago (15 km^3 yr^{-1}), to Great Britain at 13 000 yr ago (5 km^3 yr^{-1}), and finally to the remnants of the western Scandinavian ice sheet at 10 000 yr ago (10 km^3 yr^{-1}) (Fig. 10). However, by far the dominant source of meltwater was the southern margin of the ice sheet. Along this retreating margin, up to 1 500 000 km^3 of ice was melted during deglaciation. The peak meltwater production (400 km^3 yr^{-1}) occurred at 9000 yr ago, due to the rapid final-phase collapse of the Eurasian Ice Sheet.

Melting of the southern ice-sheet margin at a rate of ~100 km^3 yr^{-1} prior to the collapse of the grounded ice sheet in the southern Barents Sea may have resulted in the build up of large proglacial lakes if the ice-sheet margin was on land. However, if the glaciation of the Kara Sea was restricted, as our model shows, meltwaters from the southern region of the ice sheet could have discharged through the Kara Sea to the Arctic Ocean. Recent geological interpretation suggests the latter is likely for the last glaciation (Svendsen et al., 1999).

The process of iceberg calving was the dominant mass-loss mechanism for the last Eurasian Ice Sheet. At the LGM, iceberg production was focused at the mouths of bathymetric cross-shelf troughs, in which fast-flowing ice streams were located (Fig. 2a). The rate of iceberg calving in these regions is related to the velocity of the ice streams and the thickness of ice (i.e. the flux of ice to the continental margin).

Time-dependent variation in iceberg-calving rates at these locations (Figs. 7 and 8) shows that (1) the southernmost iceberg production zone (Norwegian Channel) was active for 4000 yr, (2) the northernmost iceberg production zones (e.g. Franz Victoria Trough) were active from 25 000 yr ago, reached a maximum at

around 15 000 yr ago, and then produced relatively few icebergs after this time, (3) iceberg production rates within the troughs west of Norway, and the Bear Island and Storfjorden troughs were maintained at high values up to 10 000 yr ago. These temporal variations in iceberg-calving rates can be explained in terms of ice-sheet decay. The ice stream within the Norwegian Channel decayed at 14 000 yr ago (as did ice in southern Scandinavia), with little iceberg calving after this time. The first phase of deglaciation in the Barents Sea caused ice streams to retreat from the continental margin after 15 000 yr ago. This caused the deglaciation of bathymetric troughs across the northern margin and, hence, the rapid reduction of iceberg flux in these regions. However, for the bathymetric troughs along the western continental margins, although the troughs may have become deglaciated, significant volumes of icebergs would have been produced in regions adjacent to the troughs because a sizeable ice sheet existed over Scandinavia and the central Barents Sea after 15 000 yr ago. The break-up of these ice sheets would have caused more iceberg calving, which would have been focused along the edge of the deglaciated troughs. Thus, icebergs would have still been released into the Norwegian–Greenland Sea at the mouths of large troughs despite the fact that they may have become deglaciated after 15 000 yr ago.

The icebergs calved from the Eurasian Ice Sheet would have floated into the neighbouring oceans. Peak rates of iceberg supply occurred at 15 000 and 12 500 ago. During the first calving peak, about 2000 km^3 yr^{-1} of icebergs were released. All the major troughs were active during this period and some (Norwegian Channel, and those in the northern Barents margin) experienced their maximum rate of calving at this time. Thus, icebergs were released into the Arctic Ocean, and the eastern margin of the Norwegian–Greenland Sea. However, at 12 500 yr ago, when the calving rate reached 1750 km^3 yr^{-1}, most icebergs were calved from Scandinavia and issued through the Bear Island Trough (from a calving front in the central Barents Sea). Thus, iceberg supply to the Arctic Ocean and southern Norwegian Sea had virtually ceased by 12 500 yr ago.

8. Conclusions

An ice-sheet model was used to construct an ice sheet across the Eurasian Arctic that was compatible with geological information relating to the maximum extent of the Late Weichselian ice sheet. An inverse-type procedure was used, where the numerical model was forced to match geological evidence through alterations to the model's environmental inputs. Once a match was made, the environmental conditions required for ice-sheet growth and decay were examined further. This approach to modelling thus allows the process of ice-sheet decay to be analysed.

- The ice sheet was initiated about 28 000 yr ago. The maximum-sized ice-sheet occupied the entire Barents Sea, Scandinavia and the North Sea. The maximum ice thickness was 2.7 km over Scandinavia and 1 km across the central Barents Sea. Fast-flowing ice streams within bathymetric troughs drained ice from the central regions of the ice sheet to the marine margin where iceberg calving occurred. No ice streams are predicted along the southern margin of the ice sheet, the extent of which was controlled by the rate of surface melting.
- During ice-sheet growth, the rate of surface melting reduced to very low values. However, the rate of iceberg calving increased steadily from 40 km^3 yr^{-1} at 25 000 yr ago to 80 km^3 yr^{-1} at 16 000 yr ago, prior to the onset of large-scale deglaciation. Deglaciation began through a dramatic increase in the rate of iceberg calving at 15 000 yr, which reached a maximum by 14 500 yr ago. During this time, the ice sheet decayed by 30%, and 750 000 km^3 of icebergs were released into the Norwegian–Greenland Sea and the Arctic Ocean. This phase of deglaciation was associated with the break-up of the deepest marine portions of the ice sheet. Another pulse of icebergs at 12 500 yr was concentrated west of Norway and the Bear Island Trough, when a further 500 000 km^3 of icebergs were calved into the Norwegian–Greenland Sea. This resulted in the ice-sheet margins retreating to the shorelines of archipelagos and land masses. In total, around 7 500 000 km^3 of icebergs were calved from the Late Weichselian Eurasian Ice Sheet.

- Distinct surface melting events were predicted across the ice sheet as the ELA rose above the ice surface due to post-LGM air-temperature rise. The first episode of meltwater production was at 14 000 yr ago due to the decay of the ice sheet over Ireland. The Great Britain ice sheet melted next at 13 000 yr, followed by the Scandinavian and other the southern regions of the ice sheet from 11 000 yr ago. In total over 1 500 000 km^3 of ice was melted from the ice sheet during the Late Weichselian deglaciation.
- In addition, the model predicts the transport of subglacial sediments to a series of known submarine fan systems (e.g. Vorren et al., 1998). Results indicate the time-dependent variation in fan build-up across the Eurasian Arctic during the Late Weichselian.
- The rate of sediment accumulation over trough-mouth fans, and the period of fan development varied spatially across the Eurasian Arctic. The North Sea Fan (at the mouth of the Norwegian Channel) experienced sediment accumulation between 18 500 and 14 500 yr ago, during which time 500 km^3 of sediment was deposited. The neighbouring fan systems off the west coast of Norway together experienced sediment build-up between 25 000 and 12 000 yr, during which time 4000 km^3 of glacigenic material was deposited.
- Two fans at the western margin of the Barents Sea were supplied with sediment between 25 000 and 12 000 yr. The largest fan (at the mouth of the Bear Island Trough) was supplied with sediment by (a) grounded ice flowing into the trough from northern Scandinavia during ice-sheet growth and (b) a fast-flowing ice stream that occupied the trough by the LGM. Around 3000 km^3 of sediment were deposited over the Bear Island Fan, whilst only 250 km^3 of sediment were deposited over the nearby Storfjorden trough-mouth fan.
- The northern Arctic Ocean margin of the Barents Shelf has four main cross-shelf troughs, including the Franz Victoria Trough (Fig. 1). The period over which sediments were deposited on this fan was somewhat less than the period of sedimentation along the western ice-sheet margin. The Franz Victoria trough-mouth fan had 500 km^3 of sediment deposited between 24 000 and 15 000 yr ago (Fig. 6b). Further east, however, the St. Anna and Voronin troughs did not contain large ice streams and, therefore, sediment supply to the continental margin was limited.

Acknowledgements

We thank Grant Bigg, Niels Reeh and Martin Jakobsson for providing constructive and helpful reviews. This work was supported by EU MAST III ENAM II Grant MAS3-CT-95-0003 to J.A.D.

References

Alley, R.B., 1990. Multiple steady states in ice-water-till systems. Ann. Glaciol. 14, 1–5.

Alley, R.B., Blankenship, D.D., Rooney, S.T., Bentley, C.R., 1989. Water-pressure coupling of sliding and bed deformation: III. Application to Ice Stream B, Antarctica. J. Glaciol. 35, 130–139.

Barnola, J.M., Raynaud, D., Korotkevich, Y.S., Lorius, C., 1987. Vostok ice core provides 160 000-year record of atmospheric CO_2. Nature 329, 408–414.

Baumann, K.H., Lackschewitz, K.S., Mangerud, J., Spielhagen, R.F., Wolf-Welling, T.C.W., Henrich, R., Kassens, H., 1995. Reflection of Scandinavian Ice Sheet fluctuations in Norwegian Sea sediments during the past 150 000 years. Quat. Res. 43, 185–197.

Bigg, G.R., Wadley, M.R., Stevens, D.P., Johnson, J.A., 1998. Simulations of two Last Glacial Maximum ocean states. Paleoceanography 13, 340–351.

Blankenship, D.D., Bentley, C.R., Rooney, S.T., Alley, R.B., 1986. Seismic measurements reveal a saturated porous layer beneath an active Antarctic ice stream. Nature 332, 54–57.

Boulton, G.S., Hindmarsh, R.C.A., 1987. Sediment deformation beneath glaciers: rheology and geological consequences. J. Geophys. Res. 92, 9059–9082.

Dowdeswell, J.A., 1995. Glaciers in the High Arctic and recent environmental change. Philos. Trans. R. Soc. London 352A, 321–334.

Dowdeswell, J.A., Siegert, M.J., 1999. Ice-sheet numerical modeling and marine geophysical measurements of glacier-derived sedimentation on the Eurasian Arctic continental margins. Geol. Soc. Am. Bull. 111, 1080–1097.

Dowdeswell, J.A., Drewry, D.J., Cooper, A.P.R., Gorman, M.R., Liestøl, O., Orheim, O., 1986. Digital mapping of the Nordaustlandet ice caps from airborne geophysical investigations. Ann. Glaciol. 8, 51–58.

Dowdeswell, J.A., Elverhøi, A., Andrews, J.T., Hebbeln, D., 1999. Asynchronous deposition of ice-rafted layers in the

Nordic seas and North Atlantic Ocean. Nature 400, 348–351.
Elverhøi, A., Solheim, A., 1983. The Barents Sea ice sheet – a sedimentological discussion. Polar Res. 1, 23–42.
Fairbanks, R.G., 1989. A 17 000-year glacio-eustatic sea level record: influence of glacial melting rates on the Younger Dryas event and deep ocean circulation. Nature 342, 637–643.
Fjeldskaar, W., 1991. Geoidal-eustatic changes induced by the deglaciation of Fennoscandia. Quat. Int. 9, 1–6.
Fjeldskaar, W., 1994. The amplitude and decay of the glacial forebulge in Fennoscandia. Nor. Geol. Tiddskr. 74, 2–8.
Fleming, K.M., Dowdeswell, J.A., Oerlemans, J., 1997. Modelling the mass balance of north-west Spitsbergen glaciers and responses to climate change. Ann. Glaciol. 24, 203–207.
Forman, S.L., Weihe, R., Lubinski, D., Tarasov, G., Korsun, S., Matishov, G., 1997. Holocene relative sea-level history of Franz Josef Land, Russia. Geol. Soc. Am. Bull. 109, 1116–1133.
Fortuin, J.P.F., Oerlemans, J., 1990. Parameterization of the annual surface temperature and mass balance of Antarctica. Ann. Glaciol. 14, 78–84.
Hanson, B., Hooke, R.L., 2000. Glacier calving: a numerical model of forces in the calving-speed–water-depth relation. J. Glaciol. 46, 188–196.
Hisdal, V., 1985. Geography of Svalbard. Polarhandbok 2. Norsk Polarinstitutt, Oslo, 75 pp.
Hughes, T.J., 1992. Theoretical calving rates from glaciers along ice walls grounded in water of variable depths. J. Glaciol. 38, 282–294.
Lambeck, K., 1995. Constraints on the Late Weichselian Ice Sheet over the Barents Sea from observations of raised shorelines. Quat. Sci. Rev. 14, 1–16.
Landvik, J.Y., Bondevik, S., Elverhøi, A., Fjeldskaar, W., Mangerud, J., Siegert, M.J., Salvigsen, O., Svendsen, J.-I., Vorren, T.O., 1998. Last glacial maximum of Svalbard and the Barents Sea area: ice sheet extent and configuration. Quat. Sci. Rev. 17, 43–75.
MacAyeal, D.R., 1992. Irregular oscillations of the West Antarctic ice sheet. Nature 359, 29–32.
Mahaffy, M.W., 1976. A three dimensional numerical model of ice sheets: tests on the Barnes Ice Cap, Northwest Territories. J. Geophys. Res. 81, 1059–1066.
Manabe, S., Bryan, K., Jr., 1985. CO_2-induced change in a coupled ocean–atmosphere model, and its paleoclimatic implications. J. Geophys. Res. 90, 11689–11707.
Mangerud, J., Svendsen, J.I., 1992. The last interglacial–glacial period on Spitsbergen, Svalbard. Quat. Sci. Rev. 11, 633–664.
Mangerud, J., Bolstad, M., Elgersma, A., Helliksen, D., Landvik, J.Y., Lønne, I., Lycke, A.K., Salvigsen, O., Sandahl, T., Svendsen, J.I., 1992. The last Glacial maximum on Spitsbergen, Svalbard. Quat. Res. 38, 1–31.
Oerlemans, J., van der Veen, C.J., 1984. Ice Sheets and Climate. Reidel, Dordrecht, 216 pp.
Paterson, W.S.B., 1994. The Physics of Glaciers, 3rd edn. Pergamon Press, Oxford.
Payne, A.J., Sugden, D.E., Clapperton, C.M., 1989. Modeling the growth and decay of the Antarctic Peninsula Ice Sheet. Quat. Res. 31, 119–134.
Pelto, M.S., Warren, C.R., 1991. Relationship between tidewater glacier calving velocity and water depth at the calving front. Ann. Glaciol. 15, 115–118.
Pelto, M.S., Higgins, S.M., Hughes, T.J., Fastook, J.L., 1990. Modeling mass-balance changes during a glaciation cycle. Ann. Glaciol. 14, 238–241.
Polyak, L., Forman, S.L., Herlihy, F.A., Ivanov, G., Krinitsky, P., 1997. Late Weichselian deglacial history of the Svyataya (Saint) Anna Trough, northern Kara Sea, Arctic Russia. Mar. Geol. 143, 169–188.
Salvigsen, O., Forman, S.L., Miller, G.H., 1992. Thermophilous molluscs on Svalbard during the Holocene and their paleoclimatic implications. Polar Res. 11, 1–10.
Siegert, M.J., 1993. Numerical Modelling Studies of the Svalbard-Barents Sea Ice Sheet. Unpubl. PhD Thesis. University of Cambridge, Cambridge, 287 pp.
Siegert, M.J., Dowdeswell, J.A., 1995. Numerical modeling of the Late Weichselian Svalbard-Barents Sea Ice Sheet. Quat. Res. 43, 1–13.
Siegert, M.J., Dowdeswell, J.A., Melles, M., 1999. Late Weichselian glaciation of the Eurasian High Arctic. Quat. Res. 52, 273–285.
Simões, J.C., 1990. Environmental Interpretation from Svalbard Ice Cores. Unpubl. PhD Thesis. University of Cambridge, Cambridge, 236 pp.
Svendsen, J.I., Astakov, V.I., Bolshiyanov, D.Y., Demidov, I., Dowdeswell, J.A., Gataullin, V., Hjort, C., Hubberten, H.W., Larsen, E., Mangerud, J., Melles, M., Möller, P., Saarnisto, M., Siegert, M.J., 1999. Maximum extent of the Eurasian ice sheets in the Barents and Kara Sea region during the Weichselian. Boreas 28, 234–242.
Tveranger, J., Astakhov, V., Mangerud, J., 1995. The margin of the last Barents-Kara Ice Sheet at Markhida, northern Russia. Quat. Res. 44, 328–340.
Vorren, T.O., Lebesbye, E., Larsen, K.B., 1990. Geometry and genesis of the glacigenic sediments in the southern Barents Sea. In: Dowdeswell, J.A., Scourse, J.D. (Eds.), Glacimarine Environments: Processes and Sediments. Geol. Soc. Spec. Publ. 53, 253–268.
Vorren, T.O., Laberg, J.S., Blaumme, F., Dowdeswell, J.A., Kenyon, N.H., Mienert, J., Rumohr, J., Werner, F., 1998. The Norwegian-Greenland Sea continental margins: Morphology and late Quaternary sedimentary processes and environment. Quat. Sci. Rev. 17, 273–302.